Journal of Sound and Vibration (2000) **235**(2), 247–260
doi:10.1006/jsvi.2000.2924, available online at http://www.idealibrary.com on IDEAL®

A HIGHER ORDER THEORY FOR STATIC–DYNAMIC ANALYSIS OF LAMINATED PLATES USING A WARPING MODEL

H. HASSIS

Ecole Nationale d'Ingénieurs de Tunis, Laboratoire Modélisation et Calcul de Structures LMCS, B.P. 37 Le Belvédère, 1002 Tunis, Tunisia. E-mail: hedi.hassis@enit.rnu.tn

(*Received* 12 *January* 1999, *and in final form* 6 *January* 2000)

A higher order theory is developed to model the behaviour of laminated plates. This theory is based on a warping theory of plate deformation developed by Hassis [1]. Through comparison with elasticity solutions obtained with classical models [2–6] and the higher order theory of Lo *et al.* [7, 8], it is shown that the present theory correctly models effects not attainable by the low order theories.

1. INTRODUCTION

A laminate consists of two or more laminate bonded together to act as an integral structural element. The laminae principal material directions are oriented to produce a structural element capable of resisting load in several directions. The stiffness of such a composite material configuration is obtained from the properties of the constituent laminae.

The classical lamination theory, often abbreviated as CLT, considers that [2–6]:

- the normal fibre to the middle surface of the laminate is assumed to remain straight (the Kirchhoff hypothesis: and perpendicular to the middle surface) when the laminate is extended and bent.
- the normal are presumed to have constant length.

The CLT uses the following field displacement, in the ($\mathbf{x}_1$, $\mathbf{x}_2$, $\mathbf{x}_3$) axes:

$$\mathbf{U}(M) = \begin{cases} U_1(x^1,\ x^2,\ x^3) = u_1(x^1, x^2) + x^3\beta_1(x^1, x^2), \\ U_2(x^1, x^2, x^3) = u_2(x^1, x^2) + x^3\beta_2(x^1, x^2), \\ U_3(x^1, x^2, x^3) = u_3(x^1, x^2), \end{cases} \tag{1}$$

where M is a point of the laminated plate, (x^1, x^2) are the middle surface co-ordinates and x^3 is the normal co-ordinate to the middle surface. (u_1, u_2, u_3) are the displacement of the mean plane written in the local plane co-ordinate, and (U_1, U_2, U_3) are the displacement of a point of the plate written in the local plane co-ordinate.

Relation (1) predicts uniform shear stress distribution and a linear one for flexural stress through the thickness of the plate.

0022-460X/00/320247 + 14 $35.00/0

Lo *et al.* [7, 8] presented a higher order theory which take the following displacement forms:

$$\begin{cases} U_1(x^1,x^2,x^3) = u_1(x^1,x^2) + x^3\beta_1(x^1,x^2) + (x^3)\zeta_1(x^1,x^2) + (x^3)^3\phi_1(x^1,x^2), \\ U_2(x^1,x^2,x^3) = u_2(x^1,x^2) + x^3\beta_2(x^1,x^2) + (x^3)^2\zeta_2(x^1,x^2) + (x^3)^3\phi_2(x^1,x^2), \\ U_3(x^1,x^2,x^3) = u_3(x^1,x^2) + x^3\beta_3(x^1,x^2) + (x^3)^2\zeta_3(x^1,x^2). \end{cases} \tag{2}$$

Lo's theory (2) was developed for homogeneous plates and extended to laminated plates.

In this work, the warping theory, developed for plates [9] and generalized to shells [1], is extended here to laminated plates.

2. DISPLACEMENT FIELD OF THE WARPING THEORY

In reference [9] a theory of plate deformation was derived which accounts for the effects of transverse shear deformation, transverse normal strain and a non-linear distribution of the in-plane displacements with respect to the thickness co-ordinate. This theory uses the normal modes associated with the normal fibre (considered as a geometrical beam) as basis functions. Using the rigid-body modes and the deformation normal modes, a higher order theory was constructed. The theory was based on the non-uniform distribution of in-plane displacement: it was called the "warping" phenomenon. In the present higher order theory, the non-uniformity of in-plane displacement of plate is considered to be a linear combination of the normal modes of the normal fibre to the mid-plane, considered as a "geometrical beam".

A higher order theory finds applications in the case of top and bottom boundary conditions of shear traction, in high-frequency dynamic analysis of plates, and in laminate plates, etc. In these cases, a higher order theory must be used because of the likely strongly non-linear thickness distribution of stresses and displacements [8, 10–14].

The warping theory takes the following displacement forms:

$$\begin{aligned} U_1(x^1,x^2,x^3) &= u_1(x^1,x^2) + x^3\beta_1(x^1,x^2) + \sum_n W_1^n(x^1,x^2)\phi_n(x^3), \\ U_2(x^1,x^2,x^3) &= u_2(x^1,x^2) + x^3\beta_2(x^1,x^2) + \sum_n W_2^n(x^1,x^2)\phi_n(x^3), \\ U_3(x^1,x^2,x^3) &= u_3(x^1,x^2) + \sum_k W_3^k(x^1,x^2)\Phi_k(x^3), \end{aligned} \tag{3}$$

where $\{\phi_n\}$ and $\{\Phi_k\}$ denote, respectively, the nth transverse and the kth longitudinal modes of vibration (see Appendix A) inducing deformations of the normal fibre which is considered as a geometrical beam.

This displacement field includes both in-plane and out-of-plane deformation modes. The functions (W_1^n, W_2^n, W_3^k) represent the intensity of the participation of the modes to warping of the normal fibre. The functions (W_1^n, W_2^n, W_3^k) are called warping co-ordinates.

Figures 1 show the first two transverse and longitudinal modes (horizontal axis) as functions of the normalized normal co-ordinate x^3/h (vertical axis). The number of modes used depends on the order of the theory needed..

3. LAMINATED PLATE THEORIES

3.1. STRESS-STRAIN BEHAVIOUR

Consider a laminated plate of thickness h, as shown in Figure 2(a), with the co-ordinate system at the mid-plane of the laminate. Each layer is orthotropic with respect to the x- and

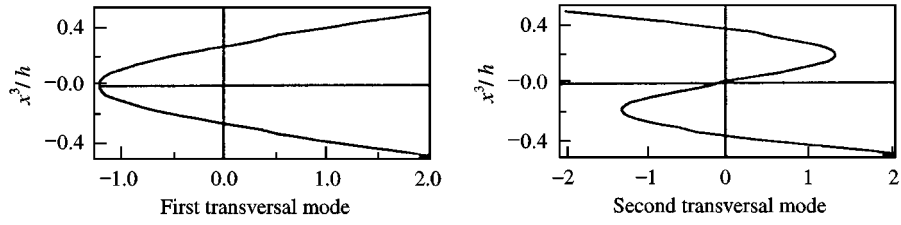

Figure 1(a). Two first transverse modes for geometrical beam associated to the normal fibre.

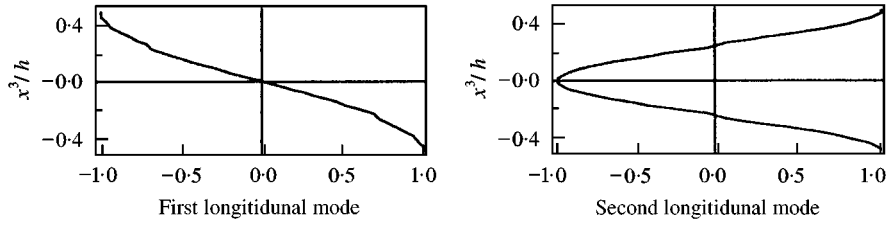

Figure 1(b). Two first longitudinal modes for geometrical beam associated to the normal fibre.

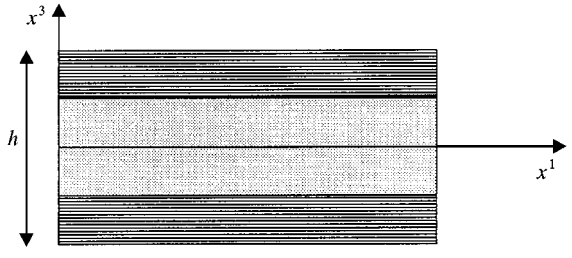

Figure 2(a) Geometry of the laminate.

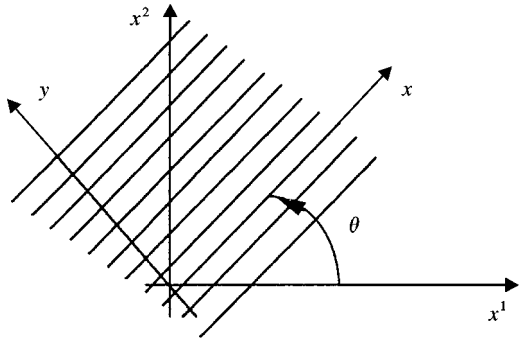

Figure 2(b). Positive rotation of principal material axes (**x**, **y**) from axes used ($\mathbf{x}^1$, $\mathbf{x}^2$).

y-axis. The fibre direction within a layer number i is indicated by an angle θ_i. The moduli of elasticity for a layer parallel to fibres is C^i_{11} and perpendicular to fibres is C^i_{22}. For each layer, the generalized Hooke's law relating stresses to strains can be written, in contracted

notation as (in the material axis x and y: see Figure 2(b))

$$\begin{bmatrix}\sigma_{xx}\\ \sigma_{yy}\\ \sigma_{zz}\\ \sigma_{xy}\end{bmatrix}=\begin{bmatrix}C_{11} & C_{12} & C_{13} & 0\\ C_{12} & C_{22} & C_{23} & 0\\ C_{13} & C_{23} & C_{33} & 0\\ 0 & 0 & 0 & C_{66}\end{bmatrix}\begin{bmatrix}\varepsilon_{xx}\\ \varepsilon_{yy}\\ \varepsilon_{zz}\\ \gamma_{xy}\end{bmatrix},\quad \begin{bmatrix}\sigma_{xz}\\ \sigma_{yz}\end{bmatrix}=\begin{bmatrix}C_{44} & 0\\ 0 & C_{55}\end{bmatrix}\begin{bmatrix}\gamma_{xz}\\ \gamma_{yz}\end{bmatrix}, \tag{4}$$

with

$$C_{11}=\frac{1-v_{23}v_{32}}{E_2E_3\Delta},\quad C_{12}=\frac{v_{21}+v_{31}v_{23}}{E_2E_3\Delta},\quad C_{13}=\frac{v_{31}+v_{21}v_{32}}{E_2E_3\Delta},$$

$$C_{22}=\frac{1-v_{13}v_{31}}{E_1E_3\Delta},\quad C_{23}=\frac{v_{32}+v_{12}v_{31}}{E_1E_3\Delta},\quad C_{33}=\frac{1-v_{12}v_{21}}{E_1E_2\Delta},$$

$$C_{44}=G_{23}=G,\quad C_{55}=G_{31},\quad C_{66}=G_{12},$$

$$\Delta=\frac{1-v_{12}v_{21}-v_{23}v_{32}-v_{31}v_{13}-{}^2v_{21}v_{32}v_{13}}{E_1E_2E_3}.$$

E_1, E_2, E_3 are, respectively, the Young moduli in x, y, and z direction and v_{ij} are the Poisson ratio for transverse strain in the j direction when stressed in the i direction.

For an arbitrary orientation defined by θ, the previous relation becomes (in the used axis $(\mathbf{x}^1, \mathbf{x}^2)$: see Figure 2(b))

$$\begin{bmatrix}\sigma_{11}\\ \sigma_{22}\\ \sigma_{33}\\ \sigma_{12}\end{bmatrix}=\begin{bmatrix}\bar{C}_{11} & \bar{C}_{12} & \bar{C}_{13} & \bar{C}_{16}\\ \bar{C}_{12} & \bar{C}_{22} & \bar{C}_{23} & \bar{C}_{26}\\ \bar{C}_{13} & \bar{C}_{23} & \bar{C}_{33} & \bar{C}_{36}\\ \bar{C}_{16} & \bar{C}_{26} & \bar{C}_{36} & \bar{C}_{66}\end{bmatrix}\begin{bmatrix}\varepsilon_{11}\\ \varepsilon_{22}\\ \varepsilon_{33}\\ \gamma_{12}\end{bmatrix},\quad \begin{bmatrix}\sigma_{13}\\ \sigma_{23}\end{bmatrix}=\begin{bmatrix}\bar{C}_{44} & \bar{C}_{45}\\ \bar{C}_{45} & \bar{C}_{55}\end{bmatrix}\begin{bmatrix}\gamma_{13}\\ \gamma_{23}\end{bmatrix}, \tag{5}$$

where $\bar{C}_{ij}$ are the components of the anisotropic stiffness matrix defined by

$$[\bar{\mathbf{C}}]=[T]^{-1}[\mathbf{C}][\mathbf{R}][\mathbf{T}][\mathbf{R}]^{-1}, \tag{6}$$

$$[\mathbf{T}]=\begin{bmatrix}\cos^2\theta & \sin^2\theta & 1 & -2\sin\theta\cos\theta\\ \sin^2\theta & \cos^2\theta & 1 & 2\sin\theta\cos\theta\\ 1 & 1 & 1 & 1\\ \sin\theta\cos\theta & -\sin\theta\cos\theta & 1 & \cos^2\theta-\sin^2\theta\end{bmatrix},\quad [\mathbf{R}]=\begin{bmatrix}1 & 0 & 0 & 0\\ 0 & 1 & 0 & 0\\ 0 & 0 & 1 & 0\\ 0 & 0 & 0 & 2\end{bmatrix} \tag{7}$$

with

$$[\mathbf{T}]^{-1}=\begin{bmatrix}\cos^2\theta & \sin^2\theta & 1 & 2\sin\theta\cos\theta\\ \sin^2\theta & \cos^2\theta & 1 & -2\sin\theta\cos\theta\\ 1 & 1 & 1 & 1\\ -\sin\theta\cos\theta & \sin\theta\cos\theta & 1 & (\cos^2\theta-\sin^2\theta)\end{bmatrix}.$$

3.2. STRAIN TENSOR

The strain tensor associated with equation (3) is written as

$$\begin{aligned}
\varepsilon_{11} &= u_{1,1} + x^3\beta_{1,1} + W^n_{1,1}\phi_n,\\
\varepsilon_{22} &= u_{2,2} + x^3\beta_{2,2} + W^n_{2,2}\phi_n,\\
2\varepsilon_{12} &= u_{1,2} + u_{2,1} + x^3(\beta_{1,2} + \beta_{2,1}) + (W^n_{1,2} + W^n_{2,1})\phi_n \quad \text{where } f,i = \frac{\partial f}{\partial x_i},\\
2\varepsilon_{13} &= \gamma_{13} = u_{3,1} + \beta_1 + W^n_1\phi_{n,3} + W^k_{3,1}\Phi_k,\\
2\varepsilon_{23} &= \gamma_{23} = u_{3,2} + \beta_2 + W^n_2\phi_{n,3} + W^k_{3,2}\Phi_k,\\
\varepsilon_{33} &= W^k_3\Phi_{k,3}.
\end{aligned} \tag{8}$$

3.3. STRESS RESULTANT

For the warping theory, the stress resultants are defined by

$$[\mathbf{N}] = \begin{bmatrix} N^{11} & N^{12}\\ N^{21} & N^{22}\end{bmatrix},\quad [\mathbf{M}] = \begin{bmatrix} M^{11} & M^{12}\\ M^{21} & M^{22}\end{bmatrix},\quad [\mathbf{P}_n] = \begin{bmatrix} P^{11}_n & P^{12}_n\\ P^{21}_n & P^{22}_n\end{bmatrix},$$
$$\mathbf{T} = \begin{pmatrix} T^1\\ T^2\end{pmatrix},\quad \mathbf{Q}^n = \begin{pmatrix} Q^1_n\\ Q^2_n\end{pmatrix},\quad \mathbf{S}^k = \begin{pmatrix} S^1_k\\ S^2_k\end{pmatrix} \tag{9}$$

with

$$\begin{bmatrix} N^{11} & N^{12} & N^{22}\\ M^{11} & M^{12} & M^{22}\\ P^{11}_n & P^{12}_n & P^{22}_n\end{bmatrix} = \int_{-h/2}^{h/2} \begin{bmatrix} 1\\ x^3\\ \phi_n\end{bmatrix} [\sigma^{11}\ \ \sigma^{12}\ \ \sigma^{22}]\,\mathrm{d}x^3,$$

$$\begin{bmatrix} T^1 & T^2\\ Q^1_n & Q^2_n\\ S^1_k & S^2_k\end{bmatrix} = \int_{-/2}^{h/2} \begin{bmatrix} 1\\ \phi_{n,3}\\ \Phi_k\end{bmatrix} [\sigma^{13}\ \ \sigma^{23}]\,\mathrm{d}x^3,\quad R_k = \int_{-h/2}^{h/2} \Phi_{k,3}\sigma^{33}\,\mathrm{d}x^3.$$

3.4. EQUATIONS OF MOTION

The governing equations pertinent to this theory are derived using the principle of virtual works in the same manner as that in reference [9]. The governing equations of motion of the warping theory are given by (see Appendix B)

$$\begin{aligned}
N^{a\lambda}_{,\lambda} + f^\alpha &= \rho h\ddot{u}^\alpha,\\
M^{\alpha\lambda}_{,\lambda} - T^\alpha + m^\alpha &= \rho\frac{h^3}{12}\ddot{\beta}^\alpha,\\
T^\alpha_{,\alpha} + f^3 &= \rho h f^3\ddot{u}_3,\\
P^{\alpha\lambda}_n + f^\alpha_n - Q^\alpha_n &= \rho h\Sigma_n\ddot{W}^\alpha_n,\\
S^\alpha_{k,\alpha} - f^3_k - R_k &= \rho h\xi_k\ddot{W}^3_k
\end{aligned} \tag{10a}$$

or

$$\operatorname{div}\mathbf{N} + \mathbf{f}_\omega = \rho h \ddot{\mathbf{u}}_\omega,$$

$$\operatorname{div}\mathbf{M} - \mathbf{T} + \mathbf{m}_\omega = \rho \frac{h^3}{12}\ddot{\boldsymbol{\beta}}$$

$$\operatorname{div}\mathbf{T} + f^3 = \rho h f^3 \ddot{u}_3, \tag{10b}$$

$$\operatorname{div}\mathbf{P}_n + \mathbf{f}_n - Q_n = \rho h \Sigma_n \ddot{\mathbf{W}}_n,$$

$$\operatorname{div}\mathbf{S}_k - f_k^3 - R_k = \rho h \xi_k \ddot{\mathbf{W}}_k^3,$$

where $\ddot{\mathbf{u}}_\omega$ is the projection on plane of the plane displacement, $\mathbf{f}_\omega$ is the in-plane forces vector, $\mathbf{m}_\omega$ is the in-plane moments vector, $\mathbf{f}_n$ is the projection of the in-plane vector forces on the nth transverse normal mode, f_k^3 is the projection of the out-of-plane force (f^3) on the kth longitudinal normal mode.

The boundary conditions are

$$-N^{\alpha\lambda}v_\lambda + f_s^\alpha = 0,$$

$$-M^{\alpha\lambda}v_\lambda + m_s^\alpha = 0,$$

$$-T^\alpha v_\alpha + f_s^3 = 0, \tag{11a}$$

$$-P_n^{\alpha\lambda}v_\lambda + (F_n^\alpha)_s = 0,$$

$$-S_k^\alpha v_\alpha + (f_k^3)_s = 0$$

or

$$-\mathbf{N}\cdot\mathbf{v} + (\mathbf{f}_\omega)_s = \mathbf{0},$$

$$-\mathbf{M}\cdot\mathbf{v} + (\mathbf{m}_\omega)_s = \mathbf{0},$$

$$-\mathbf{T}\cdot\mathbf{v} + (f^3)_s = 0, \tag{11b}$$

$$-\mathbf{P}_n\cdot\mathbf{v} + (\mathbf{f}_n)_s = \mathbf{0},$$

$$-\mathbf{S}_k\cdot\mathbf{v} - (f_k^3)_s = 0,$$

where $(\mathbf{f}_\omega)_s$ is the in-plane boundary forces vector, $(\mathbf{m}_\omega)_s$ is the in-plane boundary moments vector, $(\mathbf{f}_n)_s$ is the projection of the in-plane boundary vector forces on the nth transverse normal mode, and $(f_k^3)_s$ is the projection of the out-of-plane boundary force $(f^3)_s$ on the kth longitudinal normal mode.

Equations (11) express the equilibrium between the internal and the external forces on the boundary; for example the first equation of equation (11) expresses the equilibrium between the normal stress and the in-plane force associated with the boundary.

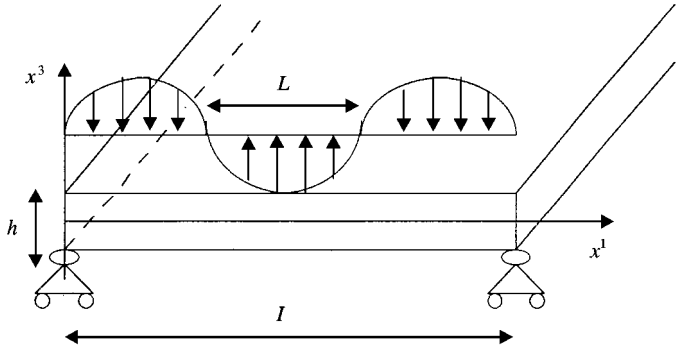

Figure 3(a). The plate considered for applications.

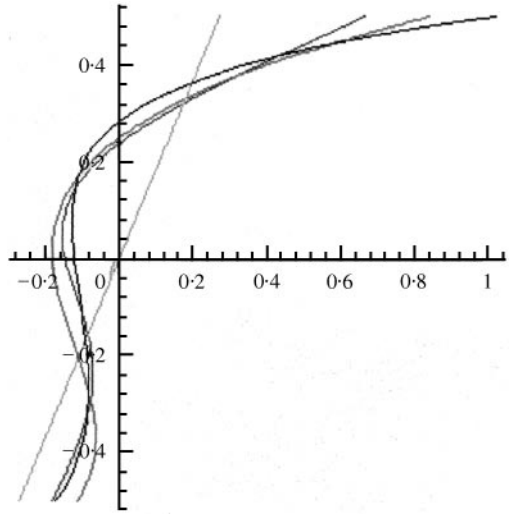

Figure 3(b). Flexural stress distribution for homogeneous plate at $h/L = 1{\cdot}5$ and for $\nu = 0{\cdot}25$: (——) Mindlin solution; (——) Lo solution; (——) warping (Hassis) solution; (——) Exact solution.

4. NUMERICAL APPLICATIONS

To validate the accuracy of the present model, a homogeneous plate and two kinds of laminated plates are considered. The first laminated plate is an angle-ply laminate and the second one is a bi-directional laminate.

For the three examples, an infinite (in x^2-direction) and a simply supported plate at $x^1 = 0$ and $x^1 = l$ is considered (l is the length of the plate). The plate is subjected to a static pressure on the top surface $x^3 = h/2$ (h is the thickness of the plate) of the form (see Figure 3(a))

$$q = q_0 \sin\left(\frac{\pi x^1}{L}\right) \tag{12}$$

with all other surface tractions identically equal to zero. L is the half wavelength of the sinusoidal loading pattern.

The problem can be solved by assuming a solution of the form

$$U_1(x^1, x^2, x^3) = \left(u_1 + x^3\beta_1 + \sum_n W_1^n \phi_n(x^3)\right)\cos\frac{\pi x^1}{L},$$
$$U_2(x^1, x^2, x^3) = \left(u_2 + x^3\beta_2 + \sum_n W_2^n \phi_n(x^3)\right)\cos\frac{\pi x^1}{L}, \tag{13a}$$
$$U_3(x^1, x^2, x^3) = \left(u_3 + \sum_n W_3^k \phi_k(x^3)\right)\sin\frac{\pi x^1}{L},$$

where u_1, β_1, W_1^n, u_2, β_2, W_2^n, u_3 and W_3^k are constants which are determined by satisfaction of the governing equations (10). The following boundary conditions (associated with equation 11) are satisfied by using the displacements (13a):

$$-N^{11} = 0, \qquad -M^{11} = 0, \quad -T^1 = 0, \quad -P_n^{11} = 0, \quad -S_k^1 = 0. \tag{13b}$$

4.1. HOMOGENEOUS PLATE

As a first validation, an homogeneous plate is considered. The flexural stress distributions across the thickness of the plate are displayed in Figure 3(b) for $h/L = 1{\cdot}5$. From Figure 3(b), it is seen that the Reissner–Mindlin solution does not come close to reproducing the exact solution. Considering the complex shape of the exact solution stress distribution, it is obvious from Figure 3(b) that the Lo *et al.* and warping solutions provide effective modelling techniques. One can note here that by considering the orthogonality between modes, the warping model is simpler than the Lo *et al.* model.

4.2. ANGLE-PLY LAMINATE

The second example is a three-layer angle-ply symmetric laminated plate. Numerical results for a three-layer symmetric laminate are shown in Figures 4–7. The ply orientation and thickness are ($+30^\circ$, -30°, $+30^\circ$) and ($h/4$, $h/2$, $h/4$) respectively. The following properties used for each ply are:

$$E_L = 25\times10^6 \text{ psi } (172{\cdot}5 \text{ GPa}), \qquad E_T = 10^6 \text{ psi } (6{\cdot}9 \text{ GPa}),$$
$$G_{LT} = 0{\cdot}5\times10^6 \text{ psi } (3{\cdot}45 \text{ GPa}), \qquad G = 0{\cdot}2\times10^6 \text{ psi } (1038 \text{ GPa}), \tag{14}$$
$$\nu_{LT} = \nu_{TT} = 0{\cdot}25,$$

where L and T are the directions parallel and normal to the fibres, respectively, and ν_{LT} is the Poisson ratio measuring transverse strain under normal stress parallel to the fibres. These are typical values of high modulus graphite/epoxy composites. The stress and displacement components in Figures 4–7 are normalized as follows:

$$\bar{u} = \frac{100\,E_T}{q_0 h S^3}u, \qquad \bar{\sigma} = \frac{\sigma}{q_0 S^2} \qquad \text{with } S = \frac{L}{h}. \tag{15}$$

Results are compared with the high order model developed by Lo *et al.* [8] and a Reissner–Mindlin solution. Results of the comparison between Lo *et al.* and the

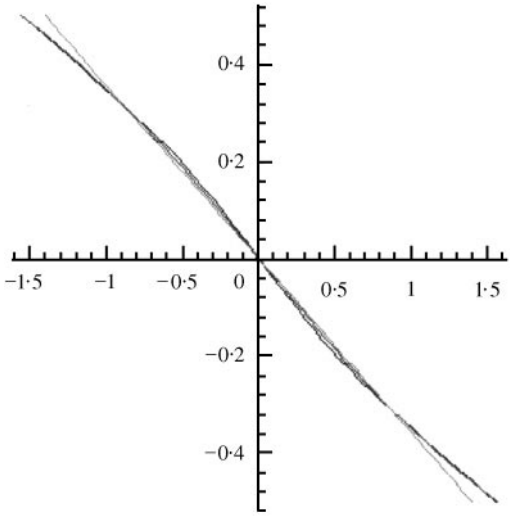

Figure 4. In-plane displacement for [+ 30°, − 30°, + 30°] angle-ply laminated at $L/h = 10$: (——) Mindlin solution; (——) Lo solution; (——) warping (Hassis) solution.

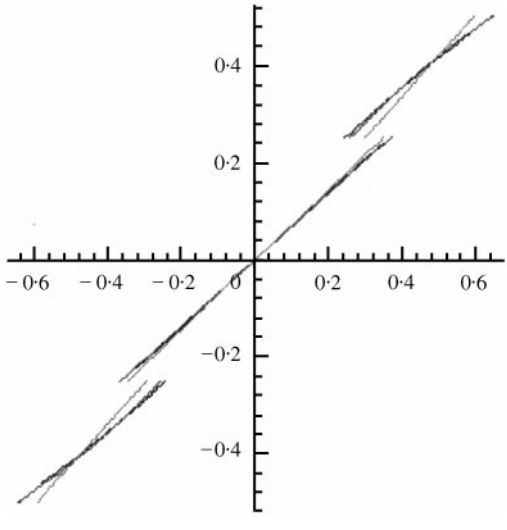

Figure 5. Flexural stress distribution for [+ 30°, − 30°, + 30°] cross-ply laminate at $L/h = 10$: (——) Mindlin solution; (——) Lo solution; (——) warping (Hassis) solution.

exact solutions can be found in Lo *et al.* [7, 8]. The exact solutions are given by Pagano [10, 11].

Figures 5 and 7 show the flexural stress distributions for the case $L/h = 10$ and 4 respectively. The agreement with Lo *et al.* solution is exceptionally good even in the region of high values of flexural stress.

Figures 4 and 6 show the corresponding in-plane displacement in the x^1 direction. As in the case of flexural stresses, good agreement with Lo *et al.* solution is observed. As mentioned in references [6, 7], these results reveal the necessity for modelling the non-linear distribution of displacements for laminated plates. The Reissner–Mindlin solution does not

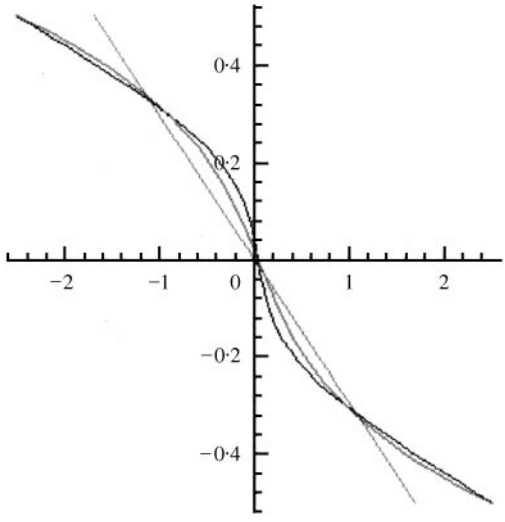

Figure 6. In-plane displacement for [+ 30°, − 30°, + 30°] angle-ply laminated at $L/h = 4$: (——) Mindlin solution; (——) Lo solution; (——) warping (Hassis) solution.

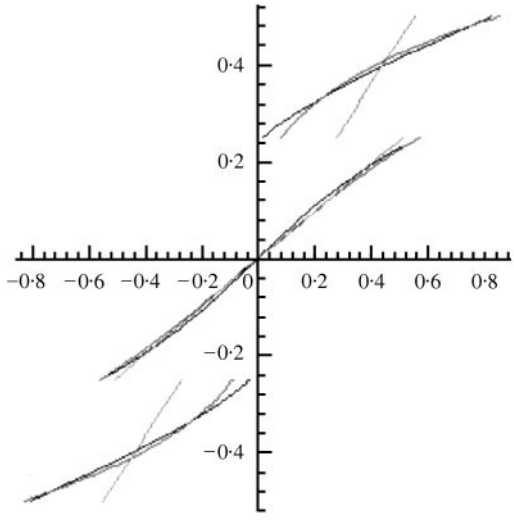

Figure 7. Flexural stress distribution for [+ 30°, − 30°, + 30°] cross-ply laminate at $L/h = 4$: (——) Mindlin solution; (——) Lo solution; (——) warping (Hassis) solution.

appear satisfactory concerning the non-uniform distribution of the normal stress and in-plane displacement.

4.3. BI-DIRECTIONAL LAMINATES

A more critical test of the laminated plate theory can be obtained by repeating the foregoing problem for a symmetric bi-directional laminate. In this case, a higher discontinuity in material properties is experienced at the interface of different layers. Numerical results for a three-layered (0°, 90°, 0°) bi-directional laminate are given in Figures

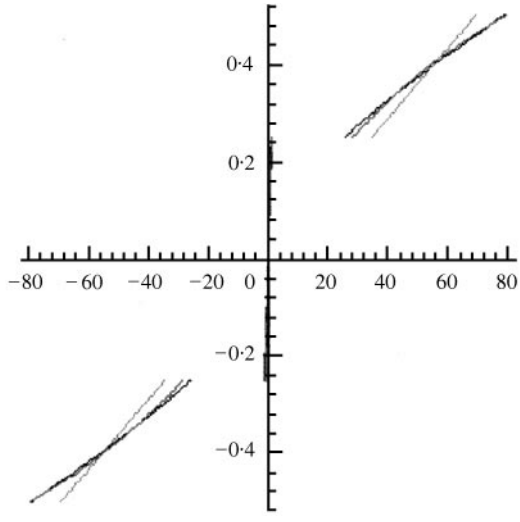

Figure 8. Flexural stress distribution for [0°, 90°, 0°] cross-ply laminate at $L/h = 10$: (~~~) Mindlin solution; (~~~) Lo solution; (~~~) warping (Hassis) solution.

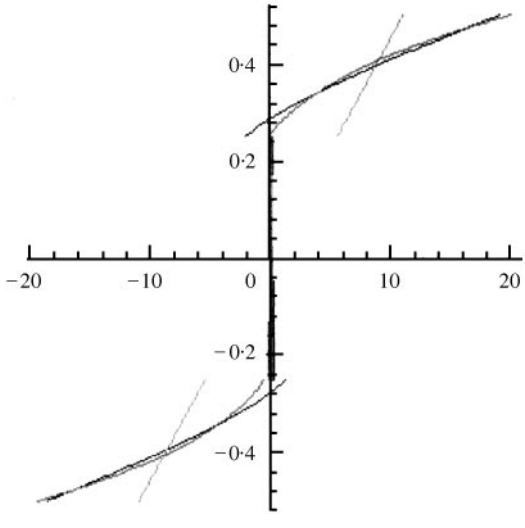

Figure 9. Flexural stress distribution for [0°, 90°, 0°] cross-ply laminate at $L/h = 4$: (~~~) Mindlin solution; (~~~) Lo solution; (~~~) warping (Hassis) solution.

8 and 9 for the flexural stress distributions. The material properties in each layer are the same as given in equation (14) and the results are compared with the higher order model developed by Lo *et al.* [8] (which is compared in reference [8] with the exact solution given by Pagano [10, 11]) and a Reissner–Mindlin solution. As in the case of angle-ply laminates, close agreement of the numerical results with exact solutions is obtained.

5. DISCUSSION–CONCLUSION

The current investigation presents an analysis of a warping model for laminated plates. The extension of the warping model to laminated plate condition is of particular

importance since it is known that for laminates the distribution of in-plane displacements across the thickness may be strongly non-linear.

By comparing the results obtained with the exact elasticity solutions, the classical laminated plate solutions and the Lo's higher order model solutions, it is obvious that the warping high order laminated plate theory gives a good approximation to the behaviour of laminated plates. The in-plane contribution to the solution has been shown to be significant and cannot be neglected. Thus, it is seen that for laminates a higher order theory of the warping type rather than classical models is required.

In the case of warping model, there is no coupling between the in-plane and the out-of-plane response. Due to the orthogonality of modes, the warping model gives simpler equations than the Lo *et al.* model.

Finally, it should be mentioned that the present results were obtained with no recourse to shear correction factors, which are commonly employed in laminated plate analysis. As discussed in reference [9], it would be inconsistent to employ these factors with a high order theory of plate deformation.

REFERENCES

1. H. HASSIS 1998 *Journal of Sound and Vibration* **225**, 633–653. A "warping-Kirchhoff" and a "warping-Mindlin" theory for shell deformation.
2. E. BOLLE 1947 *Bulletin Technique de la Suisse romande* **73**, 281–285. Contribution au problème linéaire de flexion d'une plaque élastique.
3. E. REISSNER 1945 *ASME Journal of Applied Mechanics* **12**, 69–77. The effects of transverse shear deformation on bending of elastic plates.
4. R. D. MINDLIN 1951 *ASME Journal of Applied Mechanics* **18**, 31–38. Influence of rotatory inertia and shear on flexural motions of isotropic elastic plates.
5. E. REISSNER 1975 *International Journal of Solids and Structures* **11**, 569–573. On transverse bending of plates including the effects of transverse shear deformation.
6. E. REISSNER 1985 *Applied Mechanics Review* **38**, 1453–1464. Reflections on the Theory of Elastic Plates.
7. K. H. LO, R. M. CHRISTENSEN and E. M. WU 1977 *ASME Journal of Applied Mechanics* **44**, 663–676. A high order theory of plate deformation. Part I: homogeneous plates.
8. K. H. LO, R. M. CHRISTENSEN and E. M. WU 1977 *ASME Journal of Applied Mechanics* **44**, 663–676. A high order theory of plate deformation. Part 2: laminated plates.
9. H. HASSIS 1998 *European Journal of Mechanics A/Solids* **17**, 843–853. A warping theory of plate deformation.
10. N. J. PAGANO 1969 *Journal of Composite Materials* **3**, 398–411. Exact solutions for composite laminates in cylindrical bending.
11. N. J. PAGANO 1970 *Journal of Composite Materials* **4**, 330–343. Influence of shear coupling bending of anisotropic laminates.
12. J. N. REDDY and P. H. PHAN 1985 *Journal of Sound and Vibration* **98**, 157–170. Stability and vibration of isotropic, orthotropic and laminated plates according to a higher order shear deformation theory.
13. B. N. PANDYA and T. KANT 1988 *International Journal of Solids and Structures* **24**, 1267–1278. Higher order shear deformable theories for flexural and sandwich plates Finite element evaluation.
14. A. K. NOOR and W. S. BURTON 1990 *Journal of Applied Mechanics* **57**, 182–187. Three dimensional solutions for anti symmetrically laminated anisotropic plates.

APPENDIX A

The transverse normal modes for a free–free beam are

$$\phi_n = \cos\left(\frac{\alpha_n x^3}{h}\right) + \cosh\left(\frac{\alpha_n x^3}{h}\right) - R_n\left[\sin\left(\frac{\alpha_n x^3}{h}\right) + \sinh\left(\frac{\alpha_n x^3}{h}\right)\right].$$

The coefficients α_n and R_n take the following values:

$$R_1 = 0{\cdot}9825, \quad R_2 = 1{\cdot}0008, \quad R_3 = 1{\cdot}0000, \quad R_4 = 1{\cdot}0000,$$

$$\alpha_1 = 4{\cdot}730, \quad \alpha_3 = 7{\cdot}853, \quad \alpha_3 = 10{\cdot}996, \quad \alpha_4 = 14{\cdot}137.$$

For a free–free beam, the longitudinal modes are written as follows:

$$\Phi_k = \cos\left(k\pi\left(\frac{x^3}{h} + \frac{1}{2}\right)\right).$$

APPENDIX B

For the warping model, the interior virtual work is

$$W_i = -\int_\omega \int_{-h/2}^{h/2} \sigma^{\alpha\lambda}\varepsilon_{\alpha\lambda}\,\mathrm{d}x^3\,\mathrm{d}\omega - \int_\omega \int_{-h/2}^{h/2} 2\sigma^{3\alpha}\varepsilon_{3\alpha}\,\mathrm{d}x^3\,\mathrm{d}\omega - \int_\omega \int_{-h/2}^{h/2} \sigma^{33}\varepsilon_{33}\,\mathrm{d}x^3\,\mathrm{d}\omega$$

$$= -\int_\omega \int_{-h/2}^{h/2} \sigma^{\alpha\lambda}[u_{\alpha,\lambda} + x^3\beta_{\alpha,\lambda} + W^n_{\alpha,\lambda}\,\phi_n]\,\mathrm{d}x^3\,\mathrm{d}\omega - \int_\omega \int_{-h/2}^{h/2} \sigma^{33}W^3_k\,\Phi_{k,3}\,\mathrm{d}x^3\,\mathrm{d}\omega$$

$$-\int_\omega \int_{-h/2}^{h/2} \sigma^{3\alpha}[u_{3,\alpha} + \beta_\alpha + W^n_\alpha\phi_{n,3} + W^3_{k,\alpha}\Phi_k]\,\mathrm{d}x^3\,\mathrm{d}\omega.$$

Using the stress resultant defined by equation (9), the expression of the interior virtual work becomes

$$W_i = -\int_\omega [N^{\alpha\lambda}u_{\alpha,\lambda} + M^{\alpha\lambda}\beta_{\alpha,\lambda} + P^{\alpha\lambda}_n W^n_{\alpha,\lambda}]\,\mathrm{d}\omega - \int_\omega R_k W^3_k\,\mathrm{d}\omega$$

$$-\int_\omega [T^\alpha(u_{3,\alpha} + \beta_\alpha) + Q^\alpha_n W^n_\alpha + S^\alpha_k W^3_{k,\alpha}]\,\mathrm{d}\omega.$$

After integration by parts, it becomes

$$W_i = \int_\omega [N^{\alpha\lambda}_{,\lambda}u_\alpha + M^{\alpha\lambda}_{,\lambda}\beta_\alpha + P^{\alpha\lambda}_{n,\lambda}W^n_\alpha]\,\mathrm{d}\omega - \int_\omega R_k W^3_k\,\mathrm{d}\omega$$

$$-\int_\omega [(-T^\alpha_{,\alpha}u_3 + T^\alpha\beta_\alpha) + Q^\alpha_n W^n_\alpha - S^\alpha_{k,\alpha}W^3_k]\,\mathrm{d}\omega$$

$$- \int_{\delta\omega} [N^{\alpha\lambda} u_\alpha v_\lambda + M^{\alpha\lambda} \beta_\alpha v_\lambda + P_n^{\alpha\lambda} W_\alpha^n v_\lambda] \, \mathrm{d}\Gamma$$

$$- \int_{\delta\omega} [T^\alpha u_3 v_\alpha + S_k^\alpha W_k^3 v_\alpha] \, \mathrm{d}\Gamma.$$

where v_λ is the λth component of the normal vector to the plate's boundary $\delta\omega$.

For the warping model, the exterior virtual work is (for the surface density)

$$W_e = \int_\omega [f^\alpha u_\alpha + m^\alpha \beta_\alpha + f_n^\alpha W_\alpha^n + f^3 u_3 + f_k^3 W_3^k] \, \mathrm{d}\omega$$

$$+ \int_{\delta\omega} [f_s^\alpha (u_\alpha + m_s^\alpha \beta_\alpha + (F_n^\alpha)_s W_\alpha^n + f_s^3 u_3 + (f_k^3)_s W_3^k] \, \mathrm{d}\Gamma.$$

For the warping model, the inertial virtual work is (the second order terms are neglected)

$$W_j = - \int_\omega \left[\rho h \ddot{u}^\alpha u_\alpha + \rho \frac{h^3}{12} \ddot{\beta}^\alpha \beta_\alpha + \rho h \Sigma_n \ddot{W}_n^\alpha W_\alpha^n + \rho h f^3 \ddot{u}_3 + \rho h \xi_k \ddot{W}_k^3 W_k^3 \right] \mathrm{d}\omega.$$

The application of the virtual work leads to the equilibrium equations (10) and boundary conditions (11).